Measurement of Conduction and Valence Bands g-Factors in a Transition Metal Dichalcogenide Monolayer

C. Robert,[1] H. Dery,[2,3] L. Ren,[1] D. Van Tuan,[2] E. Courtade,[1] M. Yang,[2] B. Urbaszek,[1] D. Lagarde,[1] K. Watanabe,[4] T. Taniguchi,[4] T. Amand,[1] and X. Marie[1]

[1]*Université de Toulouse, INSA-CNRS-UPS, LPCNO, 135 Avenue de Rangueil, 31077 Toulouse, France*
[2]*Department of Electrical and Computer Engineering, University of Rochester, Rochester, New York 14627, USA*
[3]*Department of Physics, University of Rochester, Rochester, New York 14627, USA*
[4]*National Institute for Materials Science, Tsukuba, Ibaraki 305-004, Japan*

(Received 6 August 2020; accepted 3 December 2020; published 10 February 2021)

The electron valley and spin degree of freedom in monolayer transition-metal dichalcogenides can be manipulated in optical and transport measurements performed in magnetic fields. The key parameter for determining the Zeeman splitting, namely, the separate contribution of the electron and hole g factor, is inaccessible in most measurements. Here we present an original method that gives access to the respective contribution of the conduction and valence band to the measured Zeeman splitting. It exploits the optical selection rules of exciton complexes, in particular the ones involving intervalley phonons, avoiding strong renormalization effects that compromise single particle g-factor determination in transport experiments. These studies yield a direct determination of single band g factors. We measure $g_{c1} = 0.86 \pm 0.1$, $g_{c2} = 3.84 \pm 0.1$ for the bottom (top) conduction bands and $g_v = 6.1 \pm 0.1$ for the valence band of monolayer WSe_2. These measurements are helpful for quantitative interpretation of optical and transport measurements performed in magnetic fields. In addition, the measured g factors are valuable input parameters for optimizing band structure calculations of these 2D materials.

DOI: 10.1103/PhysRevLett.126.067403

The effective Landé g factor of electrons, holes, and excitons in low-dimensional semiconductor systems has received considerable attention in the past 40 years since it provides precious information on the band structure [1–4]. The determination of the g-factor relies on measurement of the Zeeman energy splitting $\Delta E = g\mu_B B$, where μ_B is the electron's Bohr magneton and B is an external magnetic field which lifts the time inversion symmetry. Common techniques to measure the factor are electron spin resonance [5,6], the Hanle effect [7], magnetophotoluminescence or absorption [8], spin quantum beats [9,10], or spin flip Raman scattering [11] experiments. It was first shown by Roth *et al.* that electrons in semiconductors can have an effective g factor that differs substantially from the free-electron value $g_0 = 2$ as a consequence of the spin-orbit interaction (SOI), which couples the orbital motion with the spin degree of freedom [12].

Monolayer transition-metal dichalcogenides (ML-TMDs) are ideal two-dimensional (2D) semiconductor systems characterized by large SOI with original optoelectronic and spin or valley properties [13–15]. Magnetophotoluminescence (PL) or reflectivity measurements with out-of-plane magnetic fields were performed on ML-MoS_2, $MoSe_2$, $MoTe_2$, WS_2, and WSe_2 [16–24]. These experimental investigations yield the exciton g factors, but do not give the respective contribution linked to the conduction band (CB) and valence band (VB) g factors.

The Zeeman splitting between right and left circularly polarized light components σ^+/σ^- (defined as $E_{\sigma^+} - E_{\sigma^-} = g\mu_B B$) yields a bright exciton g factor close to $g \approx -4$ for most ML-TMDs. Surprisingly, this measured value is in agreement with a simple "atomic physics" model where the CB and VB g factors result simply from the addition of three contributions, labeled by spin, valley, and orbital terms [19,24,25]. However, the exciton g factor with this approach just reflects the contribution of the VB orbital terms. As a consequence, no decisive information can be obtained on the CB or VB g-factor values. Moreover, this simple model usually fails to predict the carrier g factors in other semiconductor structures (for instance, the well-known g factor of holes in GaAs [18]). It has indeed been shown that accurate determination of the g factor requires a precise description of the band-structure electronic states and in particular the mixing induced by the SOI [26,27]. In addition, the measurement of both CB and VB g factors (g_c and g_v) should provide valuable information on the electronic structure in ML-TMDs, for which many unknowns persist. For example, the value of the effective mass in the CB is still under debate [28–31]. The knowledge of the single particle g factor is also essential to interpret the magnetotransport experiments in which the large carrier density induces strong renormalization effects due to many-body interactions [29,32].

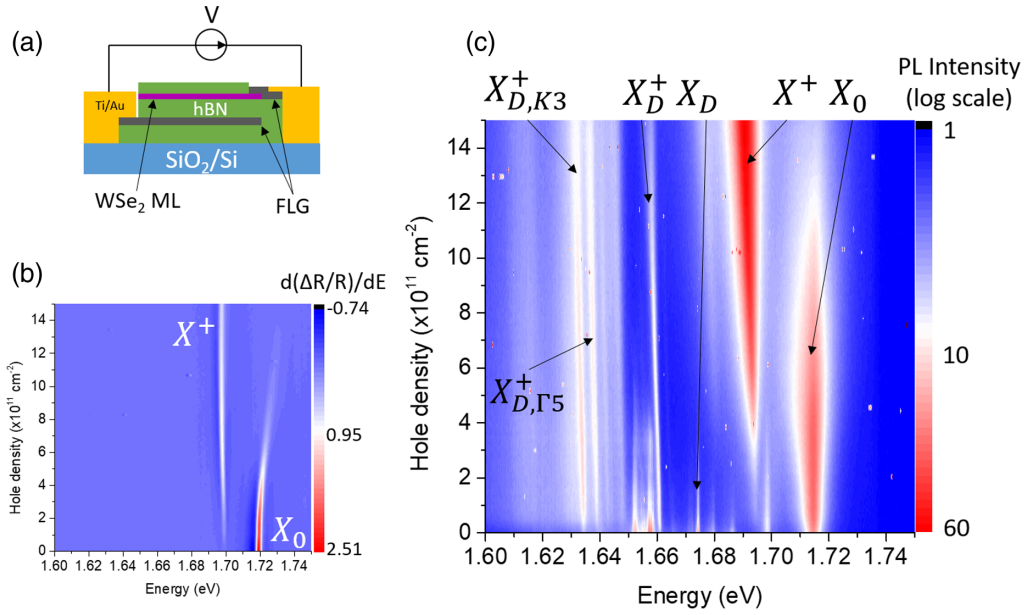

FIG. 1. (a) Sketch of the sample. A first hBN flake is exfoliated onto the $SiO_2(80\ \mathrm{nm})/Si$ substrate. Then few layers graphene (FLG) are deposited as a backgate. A second hBN flake of 140 nm is then transferred and acts as the dielectric layer of the parallel plate capacitance. Then the ML-WSe_2 is transferred and is contacted with a second FLG flake before being capped by a thin top hBN. (b) First derivative of the reflectivity contrast and (c) photoluminescence intensity as a function of hole doping for a magnetic field $B = 0$ T.

In this Letter we present magneto-PL measurements performed on a charged adjustable ML-WSe_2 sketched in Fig. 1(a). Details on the sample fabrication and experimental setup can be found in the Supplemental Material S1 [33], which includes Refs. [34–36]. We show that knowledge of the selection rules associated to optical transitions of different exciton complexes, in particular the dark positive trion and its zone-edge phonon replica, allows us to measure the g factors of the bottom CB (g_{c1}) and top VB (g_v); see Fig. 2(a). From the measured neutral exciton g factor, we can then deduce the g factor of the top CB (g_{c2}). We find $g_{c1} = 0.86 \pm 0.1$, $g_{c2} = 3.84 \pm 0.1$ and $g_v = 6.1 \pm 0.1$ in ML-WSe_2. These values differ from the predictions based on simple additive contributions of the spin, valley, and orbital components. However, our measured CB and VB g factors are in very good agreement with recent advanced density functional theory (DFT) calculations taking into account the fine characteristics of the band structure [37–39]. The experimental technique presented here to determine the g factors could be applied to other ML-TMDs in the future. Finally, we evidence a clear valley-dependent broadening of the dark positive trion PL lines, which results from Coulomb interaction between the bound trion complexes and the Fermi sea.

Experimental results.—We first present low temperature ($T = 5$ K) PL intensity and reflectivity contrast as a function of the hole doping density (tuned by the applied voltage V). The estimation of the carrier density is presented in the Supplemental Material S2 [33], which includes Ref. [40]. The neutrality region is easily identified in reflectivity when only the signature of the neutral exciton X_0 is seen [Fig. 1(b)]. When we increase the hole density, a clear signature of positively charged exciton X^+ (formed by one electron and two holes of opposite spins) is observed in agreement with previous reports [41–45]. The method presented below to determine the CB and VB g factors will be applied first in the very low doping density regime, typically $p \sim 10^{11}$ cm^{-2}, in order to avoid band-gap renormalization effects [46]. Note that this doping density is 2 orders of magnitude weaker than the critical Mott density in ML-WSe_2 [47,48]. The PL intensity plot as a function of doping in Fig. 1(c) clearly evidences exciton complex transitions already identified in the literature: in addition to the neutral bright exciton (X_0) and the positive bright trion (X^+), we observe the peaks corresponding to the neutral dark (spin forbidden) exciton X_D, the positive dark trion (X_D^+) and its phonon replicas ($X_{D,K3}^+$) and ($X_{D,\Gamma 5}^+$) [49–51], which lie 26 and 21 meV below (X_D^+), respectively. The notation of phonons K_3 and Γ_5 has its origin in the Koster notation of the K point irreducible representations of the C_{3h} point double group [52,53].

Figure 2(b) presents schematically the single-particle band structure of ML-WSe_2 at the vicinity of its CB and VB edges, along with optical selection rules associated to the radiative recombination of X_D^+ and $X_{D,K3}^+$ in an out-of-plane positive magnetic field ($B > 0$). It will allow us to present the method which yields the determination of CB and VB g factors.

Because of the interplay between SOI and the lack of inversion symmetry, absorption or emission of right and left circularly polarized light occurs in the inequivalent valleys $K+$ and $K-$ of the 2D hexagonal Brillouin zone [54–58]. The SOI yields a splitting of $\Delta_c \sim 25$ and $\Delta_v \sim 450$ meV

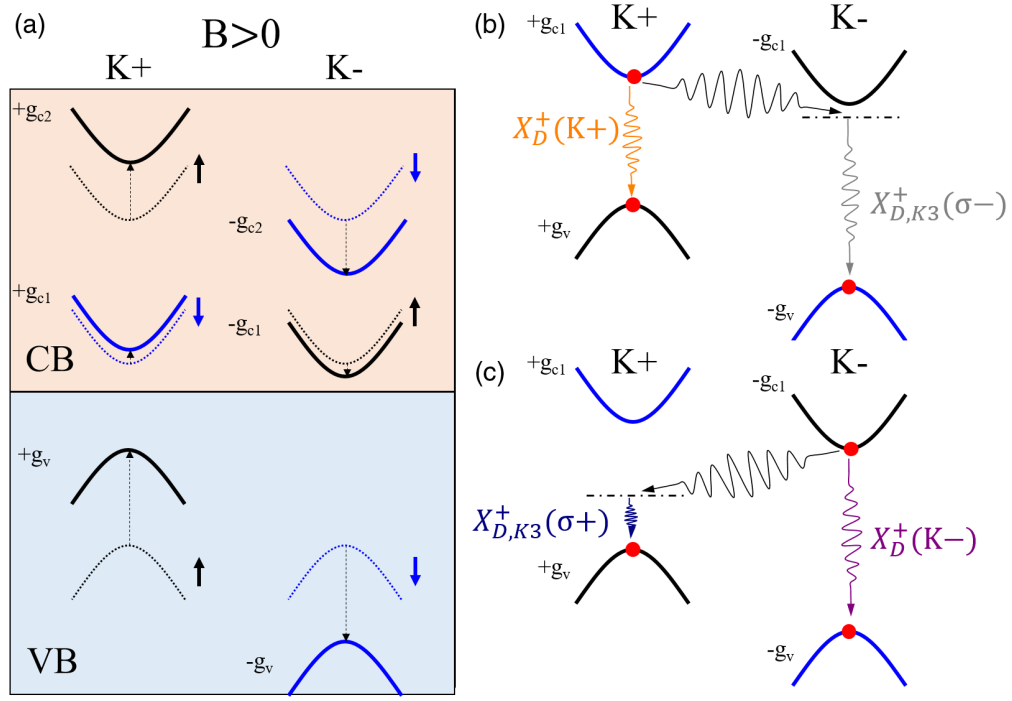

FIG. 2. (a) Schematics of the band structure in valleys $K+$ and $K-$ of ML-WSe_2 at the neutrality point; the dotted and full lines correspond to bands with $B = 0$ and $B > 0$, respectively. The vertical dotted lines indicate the magnetic field induced shift of the bands. Only the top valence band is considered here (type-A optical transitions). Schematics of the band structure for $B > 0$ and hole doping displaying the optical transition corresponding to the K_3 phonon replica of positive dark trion, $X^+_{D,K3}$, in (b) valley $K-$ and (c) valley $K+$. The optical transition of X^+_D is also indicated. The top CBs are not displayed.

between spin-up and spin-down bands in the $K+$ valley (and opposite sign values in the K valley). Here we will focus on the lowest energy transitions involving only the top VB, characterized by a g factor g_v. The bottom and top CB g factors are labeled g_{c1} and g_{c2}, respectively. The g factor of a given transition with in-plane dipole (X_0, $X^+_{D,K3}$) writes simply, $E_{\sigma+} - E_{\sigma-} = g\mu_B B$. For transitions with an out-of-plane dipole (X_D, X^+_D), the light polarization is perpendicular to the ML plane and we define the g factor by $E_{K+} - E_{K-} = g\mu_B B$ [see Figs. 2(b) and 2(c)]. For the well-known bright (X_0) and dark (X_D) neutral exciton transition, one can easily check that

$$\begin{aligned} g_{X_0} &= -2(g_v - g_{c2}) \\ g_{X_D} &= -2(g_v - g_{c1}). \end{aligned} \tag{1}$$

Figure 3(a) shows the measured transition energies for a magnetic field varying between $B = -9$ and $B = +9$ T. X_0 and X_D are measured at charge neutrality, while X^+_D and $X^+_{D,K3}$ are measured in a low p-doping regime ($p = 1.4 \times 10^{11}$ cm^{-2}). In agreement with previous reports, we find $g_{X_0} = -4.5 \pm 0.1$ and $g_{X_D} = -10.2 \pm 0.1$. As these two transitions imply two different CBs, these measurements cannot yield a determination of the CB and VB g factors [see Eq. (1)]. On the other hand, the selection rules associated with the positive dark trion optical transitions X^+_D and $X^+_{D,K3}$ allow us to solve this problem. As illustrated in Figs. 2(b) and 2(c), the positive dark trion optical transitions $X^+_D(K+)$ or $X^+_D(K-)$ denote recombination of the neutral dark exciton component and they occur between opposite VB and CB spins of the same valley (the second hole in the time-reversed valley can be considered as a "spectator"). As expected, the extracted g factor of this transition is very close to the one of the neutral dark exciton since $g_{X^+_D} = -2(g_v - g_{c1})$; we measure $g_{X^+_D} = -10.5 \pm 0.1$ [50,51].

In contrast, optical transitions that are associated with the K_3 phonon replica, $X^+_{D,K3}$, involve the second hole of the trion, which is no more a "spectator" for the optical transition [Figs. 2(b) and 2(c)] [59]. As a consequence, the energy difference between the optical transitions X^+_D and $X^+_{D,K3}$ will depend only on single band g factors g_{c1} and g_v and the energy of the phonon E_{K3}:

$$\begin{cases} \Delta E_1 = E(X^+_D(K+)) - E(X^+_{D,K3}(\sigma-)) = E_{K3} - 2g_v\mu_B B, \\ \Delta E_2 = E(X^+_D(K-)) - E(X^+_{D,K3}(\sigma+)) = E_{K3} + 2g_v\mu_B B, \\ \Delta E_3 = E(X^+_D(K-)) - E(X^+_{D,K3}(\sigma-)) = E_{K3} - 2g_{c1}\mu_B B, \\ \Delta E_4 = E(X^+_D(K+)) - E(X^+_{D,K3}(\sigma+)) = E_{K3} + 2g_{c1}\mu_B B. \end{cases} \tag{2}$$

Figure 3(b) presents the variation of $\Delta E_2 - \Delta E_1$ as a function of the applied magnetic field. The slope of the

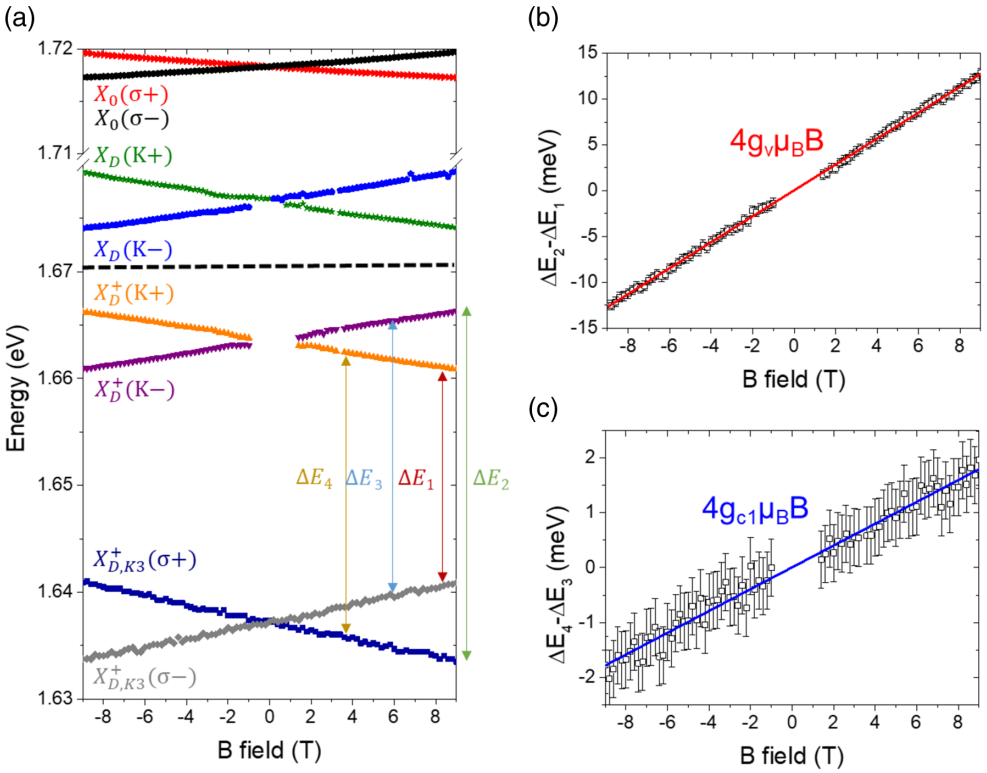

FIG. 3. (a) Magnetic field dependence of bright and dark excitons at the neutrality point of the device and positive dark trion, X_D^+, and its phonon replica involving the intervalley phonon K_3, $X_{D,K3}^+$, measured for $p = 1.4 \times 10^{11}$ cm^{-2}. Magnetic field dependence of the energy difference of the optical transitions (b) $\Delta E_2 - \Delta E_1$ and (c) $\Delta E_4 - \Delta E_3$ yielding the determination of g_v and g_{c1} [see arrows in (a)].

curve ($4g_v\mu_B$) in Fig. 3(b) yields a direct determination of the valence band g factor. We find $g_v = 6.1 \pm 0.1$. Figure 3(c) presents the magnetic field variation of the difference $\Delta E_4 - \Delta E_3$ following the same procedure. The slope gives a direct determination of the bottom CB g factor; we measure $g_{c1} = 0.86 \pm 0.1$. Then, using the measured g factor of the neutral exciton transition [Fig. 3(a) and Eq. (1)], we can deduce the top CB g factor: $g_{c2} = 3.84 \pm 0.1$. Finally, we extract the bottom VB g factor, g_{v2}, using the relation $g_{X_0,B} = -2(g_{v2} - g_{c1})$, where $g_{X_0,B}$ corresponds to the type-B neutral exciton (optical transition with in-plane dipole between bottom VB and CB). From the previously measured value of $g_{X_0,B} = -3.9 \pm 0.5$ [24], and our result for $g_{c1} = 0.86 \pm 0.1$, we get that $g_{v2} = 2.81 \pm 0.5$.

Discussion.—Zeeman splitting and corresponding g factors were calculated in ML-TMDs using DFT, tight-binding or kp approaches [37–39,60,61]. As shown in Table I, our measurements are in excellent agreement with the single-band g factors calculated recently by DFT. Despite the largest uncertainty associated to the measurement of the type-B exciton Zeeman energy that we took from Ref. [24], we note that the extracted value of the bottom VB g factor ($g_{v2} = 2.81 \pm 0.5$) is also close to the DFT calculated one (3.15) [37].

Moreover, our measurements clearly demonstrate that the simple model for calculating the g factor based on the additive contribution of the magnetic coupling to the electron spin, valley, and orbital angular momenta from the transition-metal atoms is oversimplified [19,25,62]. Though it gives a top valence band g_v value close to the measured one (5.5), it fails to predict the g factor of the CB as the simple calculation gives $g_{c2} = 3.5$ and $g_{c1} = 1.5$, assuming identical CB and VB mass ($0.4m_0$). This shows

TABLE I. Comparison of measured and calculated g factors.

	Measurements (this work)	Calculations Deilmann *et al* [37]	Calculations Woźniak *et al.* [39]	Calculations Förste *et al.* [38]	Calculations Xuan *et al.* [60]	Calculations (spin, valley, and orbital terms) [19,25]
g_{c1}	0.86	0.99	0.87	0.9	0.9	1.5
g_{c2}	3.84	3.97	3.91	3.9	3.81	3.5
g_v	6.1	5.91	5.81	5.9	5.86	5.5

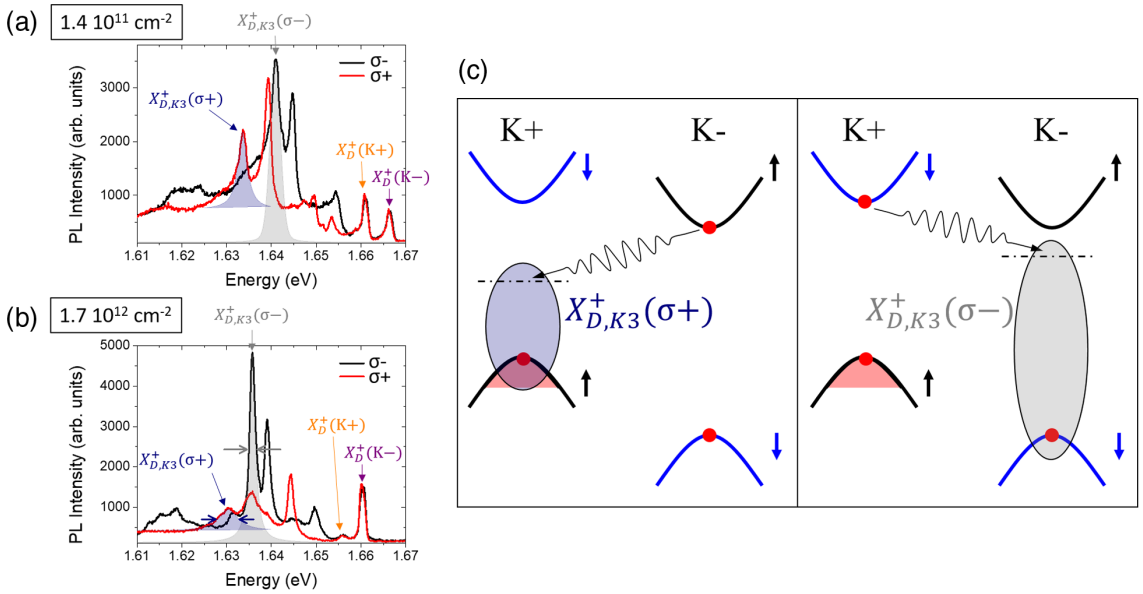

FIG. 4. Photoluminescence spectra measured at $B = 9$ T for (a) low (1.4×10^{11} cm^{-2}) and (b) large ($\sim 1.7 \times 10^{12}$ cm^{-2}) hole doping densities; (c) schematics of the optical transition associated to the K_3 phonon replica of the positive dark trion, $X^+_{D,K3}$.

that in a similar way to other semiconductors, the calculation of the g factor in ML-TMDs requires a rather detailed description of the band structure that takes into account subtle effects of the SOI [12,26,27,63,64].

Beyond the importance of the presented technique to extract the single particle g factor in the CB and VB of ML-TMDs, the results of this work merit discussion of three important points.

The first one deals with the relation between the free electron (or hole) g factor and that of excitons or trions. Our interpretation of the experiment assumes that the exciton Zeeman splitting is the sum of the Zeeman splitting energies in the CB and VB. Similar to the case of various semiconductors, we have neglected effects linked to the exciton wave function [2,63,64]. As the exciton binding energy in ML-TMDs is of the order of few hundreds meV (i.e., large extension in reciprocal space), one can question if the single-particle approach is accurate enough. Several calculations based on DFT coupled to the Bethe-Salpeter equation predicted a reduction of the exciton g factor up to 30% compared to the single-particle approach [37,60], resulting from a decrease of the magnetic moment away from the band extrema. However, we believe that the excitonic correction is negligible in ML-WSe_2 for two reasons: (i) The measured values of g factors match very well the predicted single band g factors (Table I) rather than the ones calculated with the exciton corrections. (ii) Previous measurements of the neutral exciton g factor showed that $g_n = -4.3 \pm 0.2$ for the ground and excited exciton states from $n = 1$ to $n = 4$ [65]. While these states are characterized by distinct extension in k space, their g factors are essentially the same within the experimental uncertainty.

The second point deals with the carrier-density dependence of the g factors. It is well known that exchange interactions in quantum wells of III-V semiconductors lead to enhancement of the effective g factors [66]. This enhancement has been recently evidenced in magnetotransport experiments of heavily doped ML-TMDs [32,67,68], and in Landau-quantized excitonic absorption spectroscopy of bright trions [41,69,70]. Wang *et al.* reported $g_v \sim 8.5$ and $g_{c1} \sim 4.4$ for a carrier density of $\sim 6 \times 10^{12}$ cm^{-2} in ML-WSe_2 [41], whereas Liu *et al.* found $g_v \sim 15$ and $g_{c1} \sim 2.5$ for densities larger than 10^{12} cm^{-2} [69]. In contrast, our measured values, $g_v = 6.1$ and $g_{c1} = 0.86$, show relatively little change when the gate-induced hole density changes from $\sim 10^{11}$ (Fig. 3) to 1.7×10^{12} cm^{-2} (see Supplemental Material S3, [33]), during which the corresponding Landau level filling factor at $B = 9$ T increases from $\nu < 1$ to $\nu > 6$. The reason for the disparity in the reported g-factor values remains an open question, and the relation between the energy shift of various optical transitions and exchange interactions at large doping densities is yet to be quantified. Additional work is in progress and will be presented elsewhere.

Finally, we provide evidence that trions are not readily dissociated at elevated charge densities. Figures 4(a) and 4(b) show the magneto-PL spectra at $B = 9$ T, where holes primarily populate the $K+$ valley and their densities are 1.4×10^{11} and 1.7×10^{12} cm^{-2}, respectively. Inspecting the behavior of the positive dark trion with electron in $K+$, Fig. 4(b) shows that the zero-phonon optical transition, $X^+_D(K+)$, is largely quenched. This observation is part of a universal behavior seen in semiconductors wherein optical transitions of few-body bound complexes are broadened and eventually quenched if the

spin, valley, and energy band of the recombining electron or hole are similar to those of the Fermi-sea particles (here referring to holes in the $K+$ valley). The point we wish to emphasize is that the quenched optical transition does not mean that the trion dissociates or that the trion picture is inadequate at elevated charge densities. This fact is vividly shown by comparing the optical transition, $X^{+}_{D,K3}(\sigma-)$, in Figs. 4(a) and 4(b), corresponding to the zone-edge phonon replica of the same trion. Not only that its peak amplitude is nearly 50% stronger in the higher density case, its full width at half maximum (FWHM) is narrower: ~1.7 meV at 1.7×10^{12} cm^{-2} vs ~3.4 meV at 1.4×10^{11} cm^{-2}. We attribute this counterintuitive narrowing to the longer lifetime of the trion when its recombination channels through the zero-phonon and zone-center phonon replica (Γ_5) are quenched. Thus, while the quenched behavior of $X^{+}_{D}(K+)$ may suggest that the trion is no longer bound, its phonon replica refutes this possibility. This interpretation is further supported by the opposite behavior of the positive dark trion with electron in $K-$ due to opposite labeling of the spectator and recombining holes. Here, the zero-phonon optical transition, $X^{+}_{D}(K-)$, increases in intensity when the hole density increases, whereas its zone-edge phonon replica, $X^{+}_{D,K3}(\sigma+)$, becomes weaker and its FWHM is broadened to ~5.3 meV at 1.7×10^{12} cm^{-2}. All in all, by comparing the optical transitions of the dark positive trion (zone-edge phonon replica vs the zero-phonon and/or zone-center phonon replica), we can conclude that the trions remain bound in the presence of charge carriers in ML-TMDs [71–76]. Rather than trion dissociation, the measured broadening or quenching seen in their optical transitions could be interpreted as suppressed recombination due to enhanced Coulomb scattering of the recombining hole (electron) when it has similar spin and valley quantum numbers to those of the Fermi-sea holes (electrons).

In summary, we have performed magnetophotoluminescence spectroscopy in a gated ML-WSe_2 device. Based on the knowledge of the optical selection rules of different exciton complexes, we have proposed a new method to measure the single particle g factor. Our measurements should make it possible to improve the band structure calculations in monolayer transition-metal dichalcogenides, in particular, the dispersion curves of the conduction bands which are still little known. Knowledge of the single band g factors should be valuable for understanding the properties of van der Waals heterostructures in which interlayer or moiré exciton transitions could be identified thanks to their Zeeman splitting. Finally, this work shows that by comparing optical transitions of the bare positive dark trion and its zone-edge phonon replica, one can better understand the interaction between bound trions and free charged carriers at elevated charge densities.

We thank Mathieu Pierre for his contribution to e-beam lithography. This work was supported by Agence Nationale de la Recherche funding ANR 2D-vdW-Spin, ANR VallEx, and ANR MagicValley. The work at Rochester was funded by the Department of Energy, Basic Energy Sciences, under Contract No. DE-SC0014349. X. M. also acknowledges the Institut Universitaire de France.

[1] *Optical Orientation*, edited by F. Meier and B. P. Zakharchenia (North-Holland; Elsevier Science Pub. Co, Amsterdam; New York, NY, 1984).
[2] E. L. Ivchenko, *Optical Spectroscopy of Semiconductor Nanostructures* (Alpha Science International Ltd., Harrow, 2005).
[3] D. D. Awschalom, D. Loss, and N. Samarth, *Semiconductor Spintronics and Quantum Computation* (Springer, New York, 2010).
[4] *Spin Physics in Semiconductors*, edited by M. I. Dyakonov (Springer International Publishing, Cham, 2017), Vol. 157.
[5] G. R. Johnson, A. Kana-ah, B. C. Cavenett, M. S. Skolnick, and S. J. Bass, Magnetic resonance of 2D electrons in a single quantum well of InP/GaInAs, Semicond. Sci. Technol. **2**, 182 (1987).
[6] M. Dobers, K. v. Klitzing, and G. Weimann, Electron-spin resonance in the two-dimensional electron gas of GaAs-Al_xGa_{1-x} As heterostructures, Phys. Rev. B **38**, 5453 (1988).
[7] M. J. Snelling, G. P. Flinn, A. S. Plaut, R. T. Harley, A. C. Tropper, R. Eccleston, and C. C. Phillips, Magnetic g factor of electrons in GaAs/Al_xGa_{1-x} As quantum wells, Phys. Rev. B **44**, 11345 (1991).
[8] M. Bayer, G. Ortner, O. Stern, A. Kuther, A. A. Gorbunov, A. Forchel, P. Hawrylak, S. Fafard, K. Hinzer, T. L. Reinecke, S. N. Walck, J. P. Reithmaier, F. Klopf, and F. Schäfer, Fine structure of neutral and charged excitons in self-assembled In(Ga)As/(Al)GaAs quantum dots, Phys. Rev. B **65**, 195315 (2002).
[9] A. P. Heberle, W. W. Rühle, and K. Ploog, Quantum Beats of Electron Larmor Precession in GaAs Wells, Phys. Rev. Lett. **72**, 3887 (1994).
[10] T. Amand, X. Marie, P. Le Jeune, M. Brousseau, D. Robart, J. Barrau, and R. Planel, Spin Quantum Beats of 2D Excitons, Phys. Rev. Lett. **78**, 1355 (1997).
[11] V. F. Sapega, T. Ruf, M. Cardona, K. Ploog, E. L. Ivchenko, and D. N. Mirlin, Resonant Raman scattering due to bound-carrier spin flip in GaAs/Al_xGa_{1-x} As quantum wells, Phys. Rev. B **50**, 2510 (1994).
[12] L. M. Roth, B. Lax, and S. Zwerdling, Theory of optical magneto-absorption effects in semiconductors, Phys. Rev. **114**, 90 (1959).
[13] X. Xu, W. Yao, D. Xiao, and T. F. Heinz, Spin and pseudospins in layered transition metal dichalcogenides, Nat. Phys. **10**, 343 (2014).
[14] T. Mueller and E. Malic, Exciton physics and device application of two-dimensional transition metal dichalcogenide semiconductors, npj 2D Mater. Appl. **2**, 29 (2018).
[15] G. Wang, A. Chernikov, M. M. Glazov, T. F. Heinz, X. Marie, T. Amand, and B. Urbaszek, Colloquium: Excitons in atomically thin transition metal dichalcogenides, Rev. Mod. Phys. **90**, 021001 (2018).

[16] Y. Li, J. Ludwig, T. Low, A. Chernikov, X. Cui, G. Arefe, Y. D. Kim, A. M. van der Zande, A. Rigosi, H. M. Hill, S. H. Kim, J. Hone, Z. Li, D. Smirnov, and T. F. Heinz, Valley Splitting and Polarization by the Zeeman Effect in Monolayer $MoSe_2$, Phys. Rev. Lett. **113**, 266804 (2014).

[17] A. Srivastava, M. Sidler, A. V. Allain, D. S. Lembke, A. Kis, and A. Imamoğlu, Valley Zeeman effect in elementary optical excitations of monolayer WSe_2, Nat. Phys. **11**, 141 (2015).

[18] G. Wang, L. Bouet, M. M. Glazov, T. Amand, E. L. Ivchenko, E. Palleau, X. Marie, and B. Urbaszek, Magneto-optics in transition metal diselenide monolayers, 2D Mater. **2**, 034002 (2015).

[19] G. Aivazian, Z. Gong, A. M. Jones, R.-L. Chu, J. Yan, D. G. Mandrus, C. Zhang, D. Cobden, W. Yao, and X. Xu, Magnetic control of valley pseudospin in monolayer WSe_2, Nat. Phys. **11**, 148 (2015).

[20] D. MacNeill, C. Heikes, K. F. Mak, Z. Anderson, A. Kormányos, V. Zólyomi, J. Park, and D. C. Ralph, Breaking of Valley Degeneracy by Magnetic Field in Monolayer $MoSe_2$, Phys. Rev. Lett. **114**, 037401 (2015).

[21] A. A. Mitioglu, P. Plochocka, Á. Granados del Aguila, P. C. M. Christianen, G. Deligeorgis, S. Anghel, L. Kulyuk, and D. K. Maude, Optical investigation of monolayer and bulk tungsten diselenide (WSe_2) in high magnetic fields, Nano Lett. **15**, 4387 (2015).

[22] A. Arora, R. Schmidt, R. Schneider, M. R. Molas, I. Breslavetz, M. Potemski, and R. Bratschitsch, Valley Zeeman splitting and valley polarization of neutral and charged excitons in monolayer $MoTe_2$ at high magnetic fields, Nano Lett. **16**, 3624 (2016).

[23] A. V. Stier, K. M. McCreary, B. T. Jonker, J. Kono, and S. A. Crooker, Exciton diamagnetic shifts and valley Zeeman effects in monolayer WS_2 and MoS_2 to 65 Tesla, Nat. Commun. **7**, 10643 (2016).

[24] M. Koperski, M. R. Molas, A. Arora, K. Nogajewski, M. Bartos, J. Wyzula, D. Vaclavkova, P. Kossacki, and M. Potemski, Orbital, spin and valley contributions to Zeeman splitting of excitonic resonances in $MoSe_2$ WSe_2 and WS_2 monolayers, 2D Mater. **6**, 015001 (2018).

[25] D. Xiao, W. Yao, and Q. Niu, Valley-Contrasting Physics in Graphene: Magnetic Moment and Topological Transport, Phys. Rev. Lett. **99**, 236809 (2007).

[26] M. Oestreich, S. Hallstein, A. P. Heberle, K. Eberl, E. Bauser, and W. W. Rühle, Temperature and density dependence of the electron Landé g factor in semiconductors, Phys. Rev. B **53**, 7911 (1996).

[27] W. Zawadzki, P. Pfeffer, R. Bratschitsch, Z. Chen, S. T. Cundiff, B. N. Murdin, and C. R. Pidgeon, Temperature dependence of the electron spin g factor in GaAs, Phys. Rev. B **78**, 245203 (2008).

[28] S. Larentis, H. C. P. Movva, B. Fallahazad, K. Kim, A. Behroozi, T. Taniguchi, K. Watanabe, S. K. Banerjee, and E. Tutuc, Large effective mass and interaction-enhanced Zeeman splitting of K-valley electrons in $MoSe_2$, Phys. Rev. B **97**, 201407(R) (2018).

[29] R. Pisoni, A. Kormányos, M. Brooks, Z. Lei, P. Back, M. Eich, H. Overweg, Y. Lee, P. Rickhaus, K. Watanabe, T. Taniguchi, A. Imamoglu, G. Burkard, T. Ihn, and K. Ensslin, Interactions and Magnetotransport through Spin-Valley Coupled Landau Levels in Monolayer MoS_2, Phys. Rev. Lett. **121**, 247701 (2018).

[30] A. Kormányos, G. Burkard, M. Gmitra, J. Fabian, V. Zólyomi, N. D. Drummond, and V. Fal'ko, $k \cdot p$ theory for two-dimensional transition metal dichalcogenide semiconductors, 2D Mater. **2**, 022001 (2015).

[31] M. M. Glazov, M. A. Semina, C. Robert, B. Urbaszek, T. Amand, and X. Marie, Intervalley polaron in atomically thin transition metal dichalcogenides, Phys. Rev. B **100**, 041301 (R) (2019).

[32] H. C. P. Movva, B. Fallahazad, K. Kim, S. Larentis, T. Taniguchi, K. Watanabe, S. K. Banerjee, and E. Tutuc, Density-Dependent Quantum Hall States and Zeeman Splitting in Monolayer and Bilayer WSe_2, Phys. Rev. Lett. **118**, 247701 (2017).

[33] See Supplemental Material at http://link.aps.org/supplemental/10.1103/PhysRevLett.126.067403 for a description of the experimental setup and additional data.

[34] F. Cadiz, E. Courtade, C. Robert, G. Wang, Y. Shen, H. Cai, T. Taniguchi, K. Watanabe, H. Carrere, D. Lagarde, M. Manca, T. Amand, P. Renucci, S. Tongay, X. Marie, and B. Urbaszek, Excitonic Linewidth Approaching the Homogeneous Limit in MoS_2-Based van Der Waals Heterostructures, Phys. Rev. X **7**, 021026 (2017).

[35] A. Castellanos-Gomez, M. Buscema, R. Molenaar, V. Singh, L. Janssen, H. S. J. van der Zant, and G. A. Steele, Deterministic transfer of two-dimensional materials by all-dry viscoelastic stamping, 2D Mater. **1**, 011002 (2014).

[36] T. Belhadj, C.-M. Simon, T. Amand, P. Renucci, B. Chatel, O. Krebs, A. Lemaître, P. Voisin, X. Marie, and B. Urbaszek, Controlling the Polarization Eigenstate of a Quantum Dot Exciton with Light, Phys. Rev. Lett. **103**, 086601 (2009).

[37] T. Deilmann, P. Krüger, and M. Rohlfing, Ab Initio Studies of Exciton g Factors: Monolayer Transition Metal Dichalcogenides in Magnetic Fields, Phys. Rev. Lett. **124**, 226402 (2020).

[38] J. Förste, N. V. Tepliakov, S. Y. Kruchinin, J. Lindlau, V. Funk, M. Förg, K. Watanabe, T. Taniguchi, A. S. Baimuratov, and A. Högele, Exciton g-factors in monolayer, and bilayer WSe_2 from experiment, and theory, Nat. Commun. **11**, 4539 (2020).

[39] T. Woźniak, P. E. Faria Junior, G. Seifert, A. Chaves, and J. Kunstmann, Exciton g-factors of van Der Waals heterostructures from first principles calculations, Phys. Rev. B **101**, 235408 (2020).

[40] P. Back, M. Sidler, O. Cotlet, A. Srivastava, N. Takemura, M. Kroner, and A. Imamoğlu, Giant Paramagnetism-Induced Valley Polarization of Electrons in Charge-Tunable Monolayer $MoSe_2$$, Phys. Rev. Lett. **118**, 237404 (2017).

[41] Z. Wang, J. Shan, and K. F. Mak, Valley- and spin-polarized landau levels in monolayer WSe_2, Nat. Nanotechnol. **12**, 144 (2017).

[42] S. Borghardt, B. E. Kardynał, J.-S. Tu, T. Taniguchi, and K. Watanabe, Interplay of excitonic complexes in p-doped WSe_2 monolayers, Phys. Rev. B **101**, 161402(R) (2020).

[43] Z. Ye, L. Waldecker, E. Y. Ma, D. Rhodes, A. Antony, B. Kim, X.-X. Zhang, M. Deng, Y. Jiang, Z. Lu, D. Smirnov, K. Watanabe, T. Taniguchi, J. Hone, and T. F. Heinz, Efficient

generation of neutral and charged biexcitons in encapsulated WSe_2 monolayers, Nat. Commun. **9**, 3718 (2018).
[44] M. Barbone, A. R.-P. Montblanch, D. M. Kara, C. Palacios-Berraquero, A. R. Cadore, D. De Fazio, B. Pingault, E. Mostaani, H. Li, B. Chen, K. Watanabe, T. Taniguchi, S. Tongay, G. Wang, A. C. Ferrari, and M. Atatüre, Charge-tuneable biexciton complexes in monolayer WSe_2, Nat. Commun. **9**, 3721 (2018).
[45] Z. Li, T. Wang, Z. Lu, M. Khatoniar, Z. Lian, Y. Meng, M. Blei, T. Taniguchi, K. Watanabe, S. A. McGill, S. Tongay, V. M. Menon, D. Smirnov, and S.-F. Shi, Direct observation of gate-tunable dark trions in monolayer WSe_2, Nano Lett. **19**, 6886 (2019).
[46] B. Scharf, D. Van Tuan, I. Žutić, and H. Dery, Dynamical screening in monolayer transition-metal dichalcogenides and its manifestations in the exciton spectrum, J. Phys. Condens. Matter **31**, 203001 (2019).
[47] A. Chernikov, A. M. van der Zande, H. M. Hill, A. F. Rigosi, A. Velauthapillai, J. Hone, and T. F. Heinz, Electrical Tuning of Exciton Binding Energies in Monolayer WS_2, Phys. Rev. Lett. **115**, 126802 (2015).
[48] F. Liu, M. E. Ziffer, K. R. Hansen, J. Wang, and X. Zhu, Direct Determination of Band-Gap Renormalization in the Photoexcited Monolayer MoS_2, Phys. Rev. Lett. **122**, 246803 (2019).
[49] H. Dery and Y. Song, Polarization analysis of excitons in monolayer and bilayer transition-metal dichalcogenides, Phys. Rev. B **92**, 125431 (2015).
[50] M. He, P. Rivera, D. Van Tuan, N. P. Wilson, M. Yang, T. Taniguchi, K. Watanabe, J. Yan, D. G. Mandrus, H. Yu, H. Dery, W. Yao, and X. Xu, Valley phonons and exciton complexes in a monolayer semiconductor, Nat. Commun. **11**, 618 (2020).
[51] E. Liu, J. van Baren, T. Taniguchi, K. Watanabe, Y.-C. Chang, and C. H. Lui, Valley-selective chiral phonon replicas of dark excitons and trions in monolayer WSe_2, Phys. Rev. Research **1**, 032007(R) (2019).
[52] Y. Song and H. Dery, Transport Theory of Monolayer Transition-Metal Dichalcogenides through Symmetry, Phys. Rev. Lett. **111**, 026601 (2013).
[53] G. F. Koster, J. O. Dimmock, G. Wheeler, and R. G. Satz, *Properties of Thirty-Two Point Groups* (MIT Press, Cambridge, 1963).
[54] D. Xiao, G.-B. Liu, W. Feng, X. Xu, and W. Yao, Coupled Spin and Valley Physics in Monolayers of MoS_2 and Other Group-VI Dichalcogenides, Phys. Rev. Lett. **108**, 196802 (2012).
[55] G. Sallen, L. Bouet, X. Marie, G. Wang, C. R. Zhu, W. P. Han, Y. Lu, P. H. Tan, T. Amand, B. L. Liu, and B. Urbaszek, Robust optical emission polarization in MoS_2 monolayers through selective valley excitation, Phys. Rev. B **86**, 081301(R) (2012).
[56] K. F. Mak, K. He, J. Shan, and T. F. Heinz, Control of valley polarization in monolayer MoS_2 by optical helicity, Nat. Nanotechnol. **7**, 494 (2012).
[57] T. Cao, G. Wang, W. Han, H. Ye, C. Zhu, J. Shi, Q. Niu, P. Tan, E. Wang, B. Liu, and J. Feng, Valley-selective circular dichroism of monolayer molybdenum disulphide, Nat. Commun. **3**, 887 (2012).
[58] G. Kioseoglou, A. T. Hanbicki, M. Currie, A. L. Friedman, D. Gunlycke, and B. T. Jonker, Valley polarization and intervalley scattering in monolayer MoS_2, Appl. Phys. Lett. **101**, 221907 (2012).
[59] For simplicity, the same label K3 is used for the phonon connecting the valleys K+ to K− and K− to K+ (a straightforward application of group theory should lead to the notations K3 and K2, respectively).
[60] F. Xuan and S. Y. Quek, Valley Zeeman effect and landau levels in two-dimensional transition metal dichalcogenides, Phys. Rev. Research **2**, 033256 (2020).
[61] D. V. Rybkovskiy, I. C. Gerber, and M. V. Durnev, Atomically inspired k·p approach and valley Zeeman effect in transition metal dichalcogenide monolayers, Phys. Rev. B **95**, 155406 (2017).
[62] J. R. Schaibley, H. Yu, G. Clark, P. Rivera, J. S. Ross, K. L. Seyler, W. Yao, and X. Xu, Valleytronics in 2D materials, Nat. Rev. Mater. **1**, 16055 (2016).
[63] C. Weisbuch and C. Hermann, Optical detection of conduction-electron spin resonance in GaAs, $Ga_{1-x}In_xAs$, and $Ga_{1-x}Al_xAs$, Phys. Rev. B **15**, 816 (1977).
[64] J. Hübner, S. Döhrmann, D. Hägele, and M. Oestreich, Temperature-dependent electron Landé g factor and the interband matrix element of GaAs, Phys. Rev. B **79**, 193307 (2009).
[65] A. V. Stier, N. P. Wilson, K. A. Velizhanin, J. Kono, X. Xu, and S. A. Crooker, Magnetooptics of Exciton Rydberg States in a Monolayer Semiconductor, Phys. Rev. Lett. **120**, 057405 (2018).
[66] J. Zhu, H. L. Stormer, L. N. Pfeiffer, K. W. Baldwin, and K. W. West, Spin Susceptibility of an Ultra-Low-Density Two-Dimensional Electron System, Phys. Rev. Lett. **90**, 056805 (2003).
[67] R. Pisoni, A. Kormányos, M. Brooks, Z. Lei, P. Back, M. Eich, H. Overweg, Y. Lee, P. Rickhaus, K. Watanabe, T. Taniguchi, A. Imamoglu, G. Burkard, T. Ihn, and K. Ensslin, Interactions and Magnetotransport through Spin-Valley Coupled Landau Levels in Monolayer MoS_2, Phys. Rev. Lett. **121**, 247701 (2018).
[68] M. V. Gustafsson, M. Yankowitz, C. Forsythe, D. Rhodes, K. Watanabe, T. Taniguchi, J. Hone, X. Zhu, and C. R. Dean, Ambipolar landau levels and strong band-selective carrier interactions in Monolayer WSe_2, Nat. Mater. **17**, 411 (2018).
[69] E. Liu, J. van Baren, T. Taniguchi, K. Watanabe, Y.-C. Chang, and C. H. Lui, Landau-Quantized Excitonic Absorption and Luminescence in a Monolayer Valley Semiconductor, Phys. Rev. Lett. **124**, 097401 (2020).
[70] T. Smoleński, O. Cotlet, A. Popert, P. Back, Y. Shimazaki, P. Knüppel, N. Dietler, T. Taniguchi, K. Watanabe, M. Kroner, and A. Imamoglu, Interaction-Induced Shubnikov–de Haas Oscillations in Optical Conductivity of Monolayer $MoSe_2$, Phys. Rev. Lett. **123**, 097403 (2019).
[71] *Optical Properties of 2D Systems with Interacting Electrons*, edited by W. J. Ossau and R. Suris (Springer Netherlands, Dordrecht, 2003).
[72] R. A. Sergeev and R. A. Suris, Ground-state energy of X^- and X^+ trions in a two-dimensional quantum well at an arbitrary mass ratio, Phys. Solid State **43**, 746 (2001).

[73] D. K. Efimkin and A. H. MacDonald, Many-body theory of trion absorption features in two-dimensional semiconductors, Phys. Rev. B **95**, 035417 (2017).

[74] M. Sidler, P. Back, O. Cotlet, A. Srivastava, T. Fink, M. Kroner, E. Demler, and A. Imamoglu, Fermi polaron-polaritons in charge-tunable atomically thin semiconductors, Nat. Phys. **13**, 255 (2017).

[75] D. Van Tuan, M. Yang, and H. Dery, Coulomb interaction in monolayer transition-metal dichalcogenides, Phys. Rev. B **98**, 125308 (2018).

[76] M. M. Glazov, Optical properties of charged excitons in two-dimensional semiconductors, J. Chem. Phys. **153**, 034703 (2020).